OFFICE OF NAVAL RESEARCH

CONTRACT NO. N0014–89–J–1746

R&T Code 413r001

TECHNICAL REPORT NO. 9

Reaction Rates in the Phenomenological Adiabatic Excited State Electron Transfer Theory

Keisuke Tominaga, Gilbert C. Walker, Tai Jong Kang, Paul F. Barbara and Teresa Fonseca

Submitted to

Journal of Physical Chemistry

University of Minnesota
Department of Chemistry
Minneapolis, MN 55455

May 6, 1991

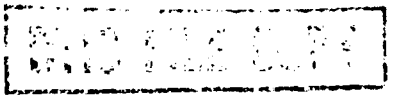

Unclassified
SECURITY CLASSIFICATION OF THIS PAGE

REPORT DOCUMENTATION PAGE

Form Approved
OMB No 0704-0188

1a REPORT SECURITY CLASSIFICATION Unclassified	1b RESTRICTIVE MARKINGS
2a SECURITY CLASSIFICATION AUTHORITY	3 DISTRIBUTION / AVAILABILITY OF REPORT Approved for public release distribution unlimited
2b DECLASSIFICATION / DOWNGRADING SCHEDULE	
4 PERFORMING ORGANIZATION REPORT NUMBER(S) Technical Report No. 9	5 MONITORING ORGANIZATION REPORT NUMBER(S)
6a NAME OF PERFORMING ORGANIZATION Department of Chemistry University of Minnesota 6b OFFICE SYMBOL (If applicable)	7a NAME OF MONITORING ORGANIZATION Office of Naval Research
6c ADDRESS (City, State, and ZIP Code) 207 Pleasant St. SE Minneapolis, MN 55455	7b ADDRESS (City, State, and ZIP Code) Chemistry Program 800 North Quincy St. Arlington, VA 22217
8a NAME OF FUNDING / SPONSORING ORGANIZATION Office of Naval Research 8b OFFICE SYMBOL (If applicable)	9 PROCUREMENT INSTRUMENT IDENTIFICATION NUMBER N0014-89-J-1746
8c ADDRESS (City, State, and ZIP Code) Chemistry Program, 800 N. Quincy St. Arlington, VA 22217	10 SOURCE OF FUNDING NUMBERS PROGRAM ELEMENT NO / PROJECT NO / TASK NO / WORK UNIT ACCESSION NO

11 TITLE (Include Security Classification)
Reaction Rates in the Phenomenological Adiabatic Excited State Electron Transfer Theory

12 PERSONAL AUTHOR(S)
Keisuke Tominaga, Gilbert C. Walker, Tai Jong Kang, Paul F. Barbara and Teresa Fonseca

13a TYPE OF REPORT	13b TIME COVERED FROM TO	14 DATE OF REPORT (Year, Month, Day)	15 PAGE COUNT
Technical		May 6, 1991	

16 SUPPLEMENTARY NOTATION

17 COSATI CODES			18 SUBJECT TERMS (Continue on reverse if necessary and identify by block number)
FIELD	GROUP	SUB-GROUP	

19 ABSTRACT (Continue on reverse if necessary and identify by block number)

See abstract on reverse side

20 DISTRIBUTION / AVAILABILITY OF ABSTRACT	21 ABSTRACT SECURITY CLASSIFICATION
☒ UNCLASSIFIED/UNLIMITED ☐ SAME AS RPT ☐ DTIC USERS	Unclassified
22a NAME OF RESPONSIBLE INDIVIDUAL Dr. Ronald A. De Marco	22b TELEPHONE (Include Area Code) / 22c OFFICE SYMBOL

DD Form 1473, JUN 86 *Previous editions are obsolete*
S/N 0102-LF-014-6603

SECURITY CLASSIFICATION OF THIS PAGE
Unclassified

19.

Abstract

The recently described phenomenological model for strongly adiabatic electron transfer (et) in the lowest excited state S_1 of donor/acceptor molecules has been developed in more detail. The model has been generalized to include simultaneously two types of electron transfer, namely adiabatic et in S_1 and diabatic et ($S_2 \rightarrow S_1$). A general definition of the et "reactant" survival probability is given in terms of the surviving charge on the donor. A relationship between the survival probability and integrated emission intensity from S_1 and S_2 is established. The use of this model is demonstrated employing the recent simulation results from our group on the excited state et of bianthryl (BA and 4-(9-anthryl)-N,N'-dimethylaniline (ADMA).

J. Phys. Chem.
4/17/91 (Submitted)

Reaction Rates in the Phenomenological Adiabatic Excited State Electron Transfer Theory

Keisuke Tominaga, Gilbert C. Walker, Tai Jong Kang,[a] Paul F. Barbara,[*]

Department of Chemistry, University of Minnesota, Minneapolis, MN 55455.

and Teresa Fonseca

Department of Chemistry, Colorado State University, Fort Collins, CO 80523.

[a] Present address: Department of Chem. Biochem., University of Texas, Austin, TX 78712.

[*] Author to whom correspondence should be addressed.

ABSTRACT

The recently described phenomenological model for strongly adiabatic electron transfer (et) in the lowest excited state S_1 of donor/acceptor molecules has been developed in more detail. The model has been generalized to include simultaneously two types of electron transfer, namely adiabatic et in S_1 and diabatic et ($S_2 \rightarrow S_1$). A general definition of the et "reactant" survival probability is given in terms of the surviving charge on the donor. A relationship between the survival probability and integrated emission intensity from S_1 and S_2 is established. The use of this model is demonstrated employing the recent simulation results from our group on the excited state et of bianthryl (BA) and 4–(9–anthryl)–N,N'–dimethylaniline (ADMA).

1. Introduction

Photophysical studies on organic aromatic electron donor/acceptor compounds are leading to new information on several issues of contemporary interest, including: the role of solvation dynamics in electron transfer (et) reactions; the mechanism of ultrafast charge separation (which is relevant to problems ranging from photosynthesis to nonlinear optics) and the effect of the solvent coordinate on the absorption and emission spectroscopy of the aromatic compounds in polar solvents.[1] The comparison between experiment and et theory has been a particular emphasis. Historically, one of the most extensively studied organic donor/acceptor compounds is 4–(9–anthryl)–N,N'–dimethylaniline (ADMA) (Figure 1).[2] The preceding article in this issue presents static and ultrafast spectroscopic data on ADMA.[3] The results are analyzed in terms of a phenomenological et model (in the strongly adiabatic regime) that was recently introduced by Kang et al. for et between strongly coupled donors and acceptors.[4]

In this paper we explore the strongly adiabatic theories in more detail. The strongly adiabatic approach is apparently a more accurate description of et between *strongly* coupled donors and acceptors than the more conventional et theories which are appropriate for weak to moderate electronic coupling.[1,5–10] It is important to note, however, that all of these theories invoke the diabatic (localized) states of Marcus theory, here denoted ψ_A and ψ_B, where A and B refer to the reactant and product states, respectively.[10] The magnitude of the interaction between the localized states is given by the electronic coupling matrix element, $H_{AB} = \int \psi_A H \psi_B d\tau$. The et kinetics are induced by fluctuations and vibrations of the nuclear coordinates, including the solvent and intramolecular vibrational modes. In the nonadiabatic and moderate adiabatic theories H_{AB} is treated by perturbation theory. In the presence of a large H_{AB} the perturbative treatment is inappropriate and a strongly adiabatic model becomes more useful. A rigorous theory of the coupling between the solvent

coordinate and the electronic coordinate in the strongly adiabatic regime has been given by Kim and Hynes.[11] Molecular dynamics simulation models that are compatible with the strongly adiabatic regime have also recently been published.[12]

For the specific case of excited state et, Tominaga et al.[3] showed the electronic coupling between the locally excited (LE) state and charge transfer (CT) state of ADMA (Figure 1) is so great that it is more useful to use the approximate[13] adiabatic states S_1 and S_2 rather than the diabatic states. Figure 2 portrays the energy dependence of the diabatic states on the displacement of the so–called solvent coordinate, z. Figure 2 shows the energy dependence of the adiabatic states which are mixtures of the diabatic states.

$$|S_1\rangle = C_{LE}^{(1)}(z)|LE\rangle + C_{CT}^{(1)}(z)|CT\rangle. \qquad (1\text{–}1)$$

$$|S_2\rangle = C_{LE}^{(2)}(z)|LE\rangle + C_{CT}^{(2)}(z)|CT\rangle. \qquad (1\text{–}2)$$

The various parameters required to construct Figure 2 were determined empirically by a phenomenological approach which involves fitting the experimental spectra to theoretical predications using the curves in Figure 2 and other information, see below and Kang et al.[4] for more details.

For ADMA the diabatic states involved in the excited state et are the LE state which results from a π–π^* transition of the anthracene ring (DA^*) and the CT state which is an intramolecular ion–pair state (D^+A^-) (Figure 1).

The ultrafast spectroscopy of ADMA shows several features which are characteristic of an adiabatic mechanism, and would be awkward to treat in a nonadiabatic representation. In particular, the fluorescence spectrum is structureless and exhibits a continuous shift of emission maximum frequency on a time scale which is approximately equal to the known

time scale for solvation dynamics, e.g. 1.7 ps in N,N–dimethylformamide.[1,6] The decay of the emission intensity is not due to loss of population of excited molecules, which occurs on a much slower time scale. The observed behavior is close to simulations using the adiabatic model. In terms of this model, the fluorescence is assigned to the S_1 state. The drop in intensity and evolution of the emission maximum frequency is assigned to diffusion along the solvation coordinate which causes the probability distribution of the solvent to evolve from its initial photoprepared distribution (peaked near $z = 0$) to its equilibrium distribution in S_1 (peaked near $z = 1$).

The decrease in intensity as the solvent coordinate evolves is due to the adiabatic et process. As the average z values goes from zero to one the amount of LE character in Ψ_{S_1} decreases, and the amount of CT character in Ψ_{S_1} increases. The transition moment ($S_1 \rightarrow S_0$) simultaneously weakens, which causes the integrated fluorescence intensity to decrease.

The S_1 adiabatic et processes of ADMA and related examples are beyond the conventional definitions of et kinetics. It is not immediately obvious how the rate coefficient (k_{et}) for this process should be defined in theoretical or experimental terms. This general problem is the main focus of the present paper. In addition, the underlying physical principals and approximations of the phenomenological adiabatic excited state et model are delineated. An additional focus of this paper is the existence of two distinct et processes, i.e. the $S_2 \rightarrow S_1$ "nonadiabatic" et mechanism and the S_1 (or S_2) adiabatic et mechanism, which were not classified in the original Kang et al.[4] paper. This paper is based primarily on simulations within the adiabatic model on ADMA and BA. Some of the simulation results have been previously discussed and shown to be in semiquantitative agreement with experiment. In the present paper, we show that the simulation results can be analyzed via a general definition of the rate coefficient to extract kinetic information on the et process.

2. The Adiabatic Electron Transfer Model and k_{et}

This section develops the basic adiabatic et model with particular emphasis on the various inherent approximations. We restrict this discussion to molecules like ADMA which involve a "two state" et process, i.e. LE → CT in a diabatic picture. The molecule BA is more complicated since there are two CT states and LE state.[4,14] However, the theoretical results for ADMA are applicable to BA with a simple extension, as will be discussed in Section 5.

For purposes of describing the excited state et of ADMA and the photodynamics of this compound, it is important to consider the S_0 ground electronic state. While this state plays a small direct role in the LE → CT et, it does play an essential role in the overall photodynamics. Optical excitation from S_0 to S_1 and S_2 prepares the t = 0 configuration of ADMA, and transient emission from the excited ADMA to S_0 is an observable which can be used to measure k_{et} and other dynamical observables (see below). For the purpose of this paper we will assume that LE and S_0 have identical charge distributions, which is consistent with experiment,[2,3] such that both states have identical equilibrium solvent configurations.

2.1. Diabatic States versus Adiabatic States

Invoking Marcus theory,[1,5–10] Tominaga et al.[3] have shown that the free energy dependence of S_0, LE, and CT should be given as follows:

$$F_{S_0}(z) = (1/2)k_s z^2, \tag{2–1}$$

$$F_{LE}(z) = (1/2)k_s z^2 + F_0, \tag{2–2}$$

$$F_{CT}(z) = (1/2)k_s(z-1)^2 + F_0 - \Delta F^0, \tag{2–3}$$

where k_s is the solvent force constant, F_0 is the energy of the spectroscopic transition between S_0 and LE, and ΔF^0 is the equilibrium free energy change for the LE → CT charge separation.

It is useful to consider approximate stationary adiabatic states for the ADMA problem as represented in Figure 2 and by eqns 1–1 and 1–2. The z dependent energies of these two states can be found approximately by diagonalizing the secular equation,

$$\begin{vmatrix} F_{LE}(z)-F & H_{LE,CT} \\ H_{LE,CT} & F_{CT}(z)-F \end{vmatrix} = 0, \qquad (2\text{–}4)$$

where the diagonalized free energies are given by eqns 2–2 and 2–3, $H_{LE,CT}$ is the electronic coupling between LE and CT, and F is the adiabatic free energy. Accordingly, the coefficients can be found by the usual means.

2.2. Electron Transfer Kinetics and the Nonadiabatic and Weak Adiabatic Theories

The basic formulation of et theory in solution is firmly routed in the localized two state description of Marcus, which involves a reactant state Ψ_R and product state Ψ_P.[10] In the language of this paper the electron that is being transferred in the reaction is first on the donor group, localized in Ψ_{LE}, and is later on the acceptor group, localized in Ψ_{CT}. As in Hückel theory, the overlap between the localized states is negligible.

$$\langle LE|CT\rangle \simeq 0. \qquad (2\text{–}5)$$

Based on this picture one can envision an operator q_D that measures the charge on the donor,

such that

$$<LE|\, q_D \,|LE> \simeq q_{el}^0, \tag{2–6}$$

$$<CT|\, q_D \,|CT> \simeq 0. \tag{2–7}$$

Thus, transitions between LE and CT physically transfer charge between the donor and acceptor. Many of the variations of contemporary et theory are based on an approximate treatment of the coupling of the nonadiabatic states to the medium fluctuation, via a Liouville equation description, that involves the diabatic states (LE and CT) as a basis set and a two state Hamiltonian:[5–10]

$$H_{el}(\epsilon) = \begin{bmatrix} \epsilon & H_{LE,CT} \\ H_{LE,CT} & \Delta E(t) \end{bmatrix}, \tag{2–8}$$

where ϵ is the energy "exchanged" with the quantum mechanical nuclear and electronic degrees of freedom, and $\Delta E(t)$ is a fluctuating energy that describes the coupling and thermal motion of the classical degrees of freedom.

The Liouville equation involves a two by two density matrix γ in the diabatic basis set, $|LE>$ and $|CT>$:

$$\frac{d\gamma(\epsilon/t)}{dt} = \frac{i}{\hbar}[H_{el}(\epsilon), \gamma(\epsilon/t)]_- - [K, \gamma(\epsilon/t)]_+. \tag{2–9}$$

Here we employ the notation $[A,B]_\pm = AB \pm BA$. K is a stochastic relaxation operator which induces relaxation in the product (CT) state.

The solution to this equation typically involves several assumptions: (i) The initial

concentration is $\gamma(\epsilon/0) = \begin{bmatrix} 1 & 0 \\ 0 & 0 \end{bmatrix} \equiv |LE\rangle$. (ii) $\Delta E(t)$ is the fluctuating energy gap, i.e. $\Delta E(t) = F_{LE}(z(t)) - F_{CT}(z(t))$ (see eqns 2–2 and 2–3), where z(t) is often assumed to obey a Fokker–Planck equation for stochastic (Brownian) solvent coordinate motion on harmonic potential. (Although we have emphasized only the solvent coordinate in the reaction coordinate, the theory can be extended to include the intramolecular vibrational motion.)

Several of the recent theoretical results on et kinetics that include the effect of solvation dynamics (and in some cases vibrational modes) are closely related to the perturbative solutions of eqn 2–9.[1,5–10] Since the physical identity of the $|LE\rangle$ and $|CT\rangle$ states is maintained in this nonadiabatic approach, the reactant survival probability is simply given for a solvent–coordinate–only model by

$$S_{NA}(t) = \int dz \rho_{LE}(z,t), \qquad (2–10)$$

where $\rho_{LE}(z,t)$ is the time–dependent classical probability distribution of the reactant in the solvent coordinate. The reaction rate coefficient is conventionally

$$k_{et}(t) = -d\ln S_{NA}(t)/dt. \qquad (2–11)$$

Note that $S_{NA}(t)$ is simply proportional to the surviving electronic charge on the donor (see eqn 2–6).

2.3. Electron Transfer Kinetics in the Strongly Adiabatic Regime

For the excited state et reactions involving a donor/acceptor pair linked by a single bond, the electronic matrix element, $H_{LE,CT}$, is large enough that the perturbative treatment in the nonadiabatic and weak adiabatic regime becomes questionable. In particular, the

degree of adiabaticity can be quantified by the adiabaticity parameter,

$$H_A = \frac{8\pi H_{LE,CT}{}^2 \tau_L}{\hbar k_s}, \qquad (2\text{–}12)$$

where τ_L is the longitudinal dielectric relation time.[7] For ADMA and BA in common polar solvents, $H_A \gg 1$ (~ 80 with $k_s = 20$ kcalmol^{-1}, $H_{LE,CT} = 1$ kcalmol^{-1}, and $\tau_L = 1$ ps), indicating that strong adiabatic effects should be considered. In addition, the adiabatic free energy surfaces for ADMA have no barrier separating the initially prepared (reactant–like) and equilibrium (product–like) regions. This is a strongly adiabatic effect which is inconsistent with a perturbative treatment of $H_{LE,CT}$. Hynes has considered strong adiabatic et reactions over a substantial barrier,[6] and related this regime to transition–state–theory. But, our concern here is small barrier[15] and barrier–free[1,9] dynamics on the adiabatic surfaces.

We have been particularly interested in an "outer–sphere" strongly adiabatic et model, which assumes that vibrational coordinates play a minor role, and treats the solvent coordinate z classically at each value of z. The system can be represented by a two by two density matrix $\Gamma(z,t)$,

$$\Gamma(z,t) = \rho(z,t) \times$$

$$\begin{pmatrix} C_{LE}^{(1)}(z)^2 + C_{CT}^{(1)}(z)^2 & C_{LE}^{(1)}(z)C_{LE}^{(2)}(z) + C_{CT}^{(1)}(z)C_{CT}^{(2)}(z) \\ C_{LE}^{(1)}(z)C_{LE}^{(2)}(z) + C_{CT}^{(1)}(z)C_{CT}^{(2)}(z) & C_{LE}^{(2)}(z)^2 + C_{CT}^{(2)}(z)^2 \end{pmatrix}. \qquad (2\text{–}13)$$

Here the off–diagonal elements are generally time–dependent and signify coherence between the S_1 and S_2 states. $\rho(z,t)$ is the classical probability of the solvent coordinate at z.

It is important to consider the properties of the off–diagonal elements. Roughly speaking, motion along z will produce coherence, i.e. non–zero off–diagonal elements. Also, the laser excitation pulse which prepares S_1 and S_2 from S_0 will create "coherence" among S_0, S_1 and S_2. However, we make the approximation that the off–diagonal terms in the adiabatic state representation are $\simeq 0$ at all relevant times. (the random phase approximation). This is appropriate where the S_1/S_2 energy gap is large enough to ensure rapid dephasing compared with the time scale for z fluctuations. Under these circumstances eqn 2–14 applies, if it is further assumed that motion along the solvent coordinate z satisfies a generalized Smoluchowski equation (GSE).[15,16] In an earlier paper we used a more exact approach involving the generalized Langevin equation (GLE) which is computationally more intensive.[4] A comparison of the GLE and GSE treatments is made in Section 5.

$$\frac{\partial\rho(z,t)}{\partial t} = D(t)\frac{\partial}{\partial z}\left(\frac{\partial}{\partial z} + \frac{1}{RT}\frac{\partial F(z)}{\partial z}\right)\rho(z,t). \qquad (2\text{–}14)$$

Here D(t) and F(z) are a generalized diffusion coefficient and a potential acting on the system, respectively.

$$\frac{\partial\rho_{S_1}(z,t)}{\partial t} = D(t)\frac{\partial}{\partial z}\left(\frac{\partial}{\partial z} + \frac{1}{RT}\frac{\partial F_{S_1}(z)}{\partial z}\right)\rho_{S_1}(z,t) - k_{S_1\to S_2}(z)\rho_{S_1}(z,t) + k_{S_2\to S_1}(z)\rho_{S_2}(z,t). \qquad (2\text{–}15)$$

$$\frac{\partial\rho_{S_2}(z,t)}{\partial t} = D(t)\frac{\partial}{\partial z}\left(\frac{\partial}{\partial z} + \frac{1}{RT}\frac{\partial F_{S_2}(z)}{\partial z}\right)\rho_{S_2}(z,t) + k_{S_1\to S_2}(z)\rho_{S_1}(z,t) - k_{S_2\to S_1}(z)\rho_{S_2}(z,t). \qquad (2\text{–}16)$$

Here $k_{S_2 \to S_1}(z)$ and $k_{S_1 \to S_2}(z)$ are defined as diabatic rate constants and represent "internal conversion" between S_1 and S_2. In this paper we leave the form of these internal conversion mechanisms unspecified. They are physically analogous to the radiationless decay between states of the same spin multiplicity, and, as such, formally represent a non–Born–Oppenheimer transition of state. In order to simulate the overall dynamics in terms of eqns 2–15 and 2–16, initial distributions of $\rho_{S_1}(z,t)$ and $\rho_{S_2}(z,t)$ are required, and values for the various parameters, $D(t)$, k_s, ..., etc. are needed The methods for performing such simulations from phenomenological estimates have been outlined previously by Kang et al.[4] and Tominaga et al.,[3] and will also be discussed below.

Our major interest here, however, is a "reactant" survival probability and, in turn, a definition for k_{et} that is appropriate in all et regimes including the strongly adiabatic limit. The definition of the survival probability follows from the definition of the operator q_D (eqns 2–6 and 2–7). The expectation value of this operator for the system wavefunction (according to the random phase approximation) can be shown to be

$$\int dz \langle \Psi_{sys} | q_D | \Psi_{sys} \rangle = q_{el}^0 [\int \rho_{S_1}(z,t) C_{LE}^{(1)}(z)^2 dz + \int \rho_{S_2}(z,t) C_{LE}^{(2)}(z)^2 dz]. \tag{2–17}$$

Thus, the "generalized" survival $S_G(t)$ of the electronic charge on the donor divided by the charge of an electron q_{el}^0 is

$$S_G(t) = \int dz [\rho_{S_1}(z,t) C_{LE}^{(1)}(z)^2 + \rho_{S_2}(z,t) C_{LE}^{(2)}(z)^2]$$

$$= [\overline{C_{LE}^{(1)\,2}(t)} + \overline{C_{LE}^{(2)\,2}(t)}] \cdot N_T \tag{2–18},$$

where the rhs of eqn 2–18 represents the z–averaged probability of the LE character times the total number N_T of S_1 and S_2 molecules, N_{S_1} and N_{S_2}, respectively.

$$N_T = N_{S_1} + N_{S_2}. \tag{2–19}$$

$$N_{S_1} = \int dz \rho_{S_1}(z,t). \tag{2–20}$$

$$N_{S_2} = \int dz \rho_{S_2}(z,t). \tag{2–21}$$

An average of a function of z, $C_x^{(i)}(z)$, over z on the S_i surface at time t is defined as

$$\overline{C_x^{(i)}(t)} = [\int dz \rho_{S_i}(z,t) C_x^{(i)}(z)]/[\int dz \rho_{S_1}(z,t) + \int dz \rho_{S_2}(z,t)], \tag{2–22}$$

where i=1 or 2 and x = LE or CT. In turn, the generalized et rate coefficient, $k_{et}(t)$, can be expressed as

$$k_{et}(t) = -d\ln(S_G(t) - S_G(\infty))/dt. \tag{2–23}$$

This expression is analogous to the conventional definition of a reaction rate constant in terms of a surviving "concentrations" of the reactants. $S_G(\infty)$ is the equilibrium value of the survival of the electronic charge. In the case of the adiabatic model, $S_G(\infty)$ is the thermally average LE character at equilibrium. By analogy to conventional reactions, if $S_G(\infty)$ is approximately zero, the adiabatic et reaction is effectively irreversible. In contrast, a non–zero $S_G(\infty)$ signifies a reversible et reaction, which is the case for the S_1 et reaction of

ADMA (see below).

Having defined a general survival, we now turn to its relationship to experimental observables. The key observable is the integrated emission intensity

$$A(t) \propto \int d\nu I(t,\nu)/\nu^3, \tag{2–24}$$

where $I(t,\nu)$ is the time–dependent fluorescence spectrum to S_0 from both S_1 and S_2 (within the random phase approximation). An expression for $A(t)$ in terms of $S_G(t)$ can be derived by simple manipulations of the basic photodynamic equations of the Kang et al. model. $A(t)$ is proportional to the square of the expectation value of the electronic transition dipole moment operator μ (within the Franck–Condon approximation).

$$A(t) \propto \int dz |\langle \Psi_{sys}|\mu|S_0\rangle|^2 \tag{2–25}$$

$$\propto \int dz[\rho_{S_1}(z,t)|\langle S_1|\mu|S_0\rangle|^2 + \rho_{S_2}(z,t)|\langle S_2|\mu|S_0\rangle|^2]. \tag{2–26}$$

The z dependent contribution to the transition moment is given by

$$\langle S_i|\mu|S_0\rangle = C_{LE}^{(i)}(z)\mu_{LE} + C_{CT}^{(i)}(z)\mu_{CT}, \tag{2–27}$$

where i = 1 or 2 and μ_{LE} and μ_{CT} are the dipole transition moments connecting the diabatic states,

$$\mu_{LE} = \langle LE|\mu|S_0\rangle, \tag{2–28}$$

$$\mu_{CT} = \langle CT|\mu|S_0\rangle. \tag{2-29}$$

Utilizing the definition in eqn 2–22 of the average of $C_x^{(i)}$ over the solvent coordinate at time t, it is useful to make the approximation that the average of the square is approximately equal to the square of the average, i.e.

$$\overline{C_{LE}^{(i)2}(t)} \simeq [\overline{C_{LE}^{(i)}(t)}]^2, \tag{2-30}$$

and similarly

$$\overline{C_{LE}^{(i)} C_{CT}^{(i)}(t)} \simeq \overline{C_{LE}^{(i)}(t)} \cdot \overline{C_{CT}^{(i)}(t)}. \tag{2-31}$$

In a latter section of this paper we examine the range of validity of this approximation using the simulation results.

The integrated emission intensity A(t) can be related to $C_{LE}^{(i)}$ and $C_{CT}^{(i)}$ by the following expression from eqns 2–26 and 2–27

$$A(t) \propto \overline{(C_{LE}^{(1)}\mu_{LE} + C_{CT}^{(1)}\mu_{CT})^2(t)} + \overline{(C_{LE}^{(2)}\mu_{LE} + C_{CT}^{(2)}\mu_{CT})^2(t)}, \tag{2-32}$$

If all the population on S_2 relaxes to the S_1 surface due to the fast internal conversion, A(t) can be related to $S_G(t)$ in a simple way, using eqns 2–18, 2–30, 2–31,2–32 and $\overline{(C_{LE}^{(i)}(t))^2} + \overline{(C_{CT}^{(i)}(t))^2} \simeq 1$,

$$S_G(t) \simeq [\mu_{LE}\sqrt{B(t)} - \mu_{CT}\sqrt{\mu_{LE}^2+\mu_{CT}^2-B(t)}]/(\mu_{LE}^2 + \mu_{CT}^2)^2, \tag{2–33}$$

where

$$B(t) = \frac{A(t)}{A(\infty)}(\overline{C_{LE}^{(1)}(\infty)}\mu_{LE} + \overline{C_{CT}^{(1)}(\infty)}\mu_{CT})^2, \tag{2–34}$$

where we used $N_T = 1$ (slow population depletion process compared with the et reaction).

This expression is a general definition for the survival in all regimes from the weakly adiabatic to the strongly adiabatic, within the previously noted approximations.

The situation is particularly simple in the *non–adiabatic limit* for which the weak coupling between the donor and acceptor ensures that $\mu_{LE} \gg \mu_{CT}$. In this limit, the optical excitation pulse prepares a pure LE state, and only LE $\rightarrow S_0$ emission can be observed. Under these circumstances eqn 2–33 reduces to eqn 2–10.

$$S_G(t) \propto A(t)_{LE\rightarrow S_0} \propto S_{NA}(t), \tag{2–35}$$

which means that the integrated emission intensity directly monitors the LE concentration. Furthermore, in the nonadiabatic regime if the reactant and product wells are divided by a large activation barrier, the survival can be simply measured by monitoring the emission intensity at a single wavelength region

$$S_G(t) \propto I(t,\nu). \tag{2–36}$$

For the strongly adiabatic limit eqns 2–35 and 2–36 are not generally valid. Indeed they very poorly describe the situation for ADMA. On the other hand, eqns 2–35 and 2–36 can be approximately valid in the strongly adiabatic limit if a large activation barrier is present. Under this situation, the shape of $\rho(z,t)$ in the reactant "well" can be approximately time–invariant. These issues should become clearer as we consider specific simulation of the excited state et dynamics of ADMA and BA.

3. An Approximate Expression of $k_{et}(t)$ in the Strongly Inverted Regime

Ultrafast laser studies have been made for BA, ADMA, and related compounds. In the case of BA the excitation wavelength in these studies exclusively prepares the S_1 state. For ADMA, both S_1 and S_2 are prepared by the laser excitation, but the S_2 state is converted to S_1 within < 150 fs. Thus, for both compounds, the et process occurs predominantly in the S_1 state. For et in the S_1 state only, eqn 2–18 reduces to

$$S_G(t) = \int dz \rho_{S_1}(z,t) C_{LE}^{(1)}(z)^2. \qquad (3–1)$$

The functional form of $C_{LE}^{(1)}(z)$ is obtained by solving the secular equation (eqn 2–4). For example,

$$C_{LE}^{(1)}(z)^2 = 2H_{LE,CT}{}^2 \times [4H_{LE,CT}{}^2 + \Delta F(z)^2 + \Delta F(z)\sqrt{\Delta F(z)^2 + 4H_{LE,CT}{}^2}\,]^{-1}, \qquad (3–2)$$

where $\Delta F(z)$ is free energy difference between the LE and CT states, and

$$\Delta F(z) = F_{LE}(z) - F_{CT}(z)$$

$$= k_s(z - 1/2) + \Delta F^0. \qquad (3\text{–}3)$$

In general, $S_G(t)$ and correspondingly $k_{et}(t)$ can be calculated by first employing the GSE and GLE to calculate $\rho(z,t)$ from a given initial condition $\rho(z,t=0)$. The procedure is outlined elsewhere.[3,4]

In order to establish a basic physical understanding of $S_G(t)$ and $k_{et}(t)$ it is useful to consider an approximate analytical expression for these questions in the limit of a strongly inverted et reaction, such as ADMA. In this limit, $F_{S_1}(z)$ has a single minimum at $z = 1$, and is approximately equal to $F_{CT}(z)$ near the $z = 1$ minimum, i.e. $F_{S_1}(z)$ is harmonic near $z = 1$ as shown in Figures 2 and 3. It will be shown below that at late times $\rho(z,t)$ is approximately Gaussian with a maximum position $\hat{z} \simeq 0.95$, that is approximately the equilibrium value, $\hat{z} = 1$, see the bottom panel in Figure 3. Under these circumstances a solution to eqn 2–14 for a harmonic potential leads to the following expression for $\hat{z}$,

$$\hat{z}(t) \simeq 1\text{–}\exp(-t/\tau_s), \qquad (3\text{–}4)$$

where it has been assumed that the solvation dynamics are overdamped and well characterized by a single relaxation time τ_s. Eqn 3–4 is the same result found in the derivation of the so–called transient Stokes shift.[1]

Assuming that the shape of $\rho(z,t)$ is slowly varying on the time scale of τ_s, which is a result of the simulation (Figure 3), we can replace the integral in eqn 2–18 by the following expression,

$$S_G(t) \simeq C_{LE}^{(1)}(\hat{z}(t))^2, \qquad (3\text{–}5)$$

which should apply at long times.

Combining eqns 3–2, 3–4, 3–5, and the definition of $k_{et}(t)$ in terms of $S_G(t)$ (eqn 2–23), it is easy to show that the limiting rate coefficient,

$$k_{et}^{lim} \equiv \lim_{t\to\infty} k_{et}(t)$$

$$= \lim_{t\to\infty} [-\frac{d}{dt}\ln(S_G(t) - S_G(\infty))], \qquad (3\text{–}6)$$

leads to

$$k_{et}^{lim} = 1/\tau_s. \qquad (3\text{–}7)$$

This relationship indicates that for adiabatic et reaction in the strongly inverted regime, solvation dynamics are rate limiting, which is closely related to analogous results from the weakly adiabatic model.[1,5–10]

4. The S_1 Adiabatic ET Kinetics of ADMA

Tominaga et al.[3] have reported transient emission data $I(\nu,t)$ on ADMA in the polar aprotic solvent N,N–dimethylformamide (DMF) which according to transient Stokes shift measurements[1.b] has an average solvation time $<\tau_s>$ of 1.0 – 1.5 ps. The experimental $I(t,\nu)$ results are very similar to simulations of the spectra using strongly adiabatic model, as shown in Figure 4. The simulations in Figure 4 have been described previously.[3,4] They involve a convolution of an empirical spectral shape function with $\rho(z,t)$,

$$I(t,\nu) \propto \int dz |\langle S_1|\mu|S_0\rangle|^2 g(\nu_0(z),\nu-\nu_0(z))\rho(z,t)\nu^3, \tag{4-1}$$

where $g(\nu_0(z),\nu-\nu_0(z))$ the normalized emission spectral shape and $\nu_0(z)$ corresponds to the free energy difference between the S_1 and S_0 states, $\nu_0(z) = (F_{S_1}(z) - F_{S_0}(z))/h$. Here $\rho(z,t)$ was calculated numerically[3] from eqn 2–14 using an initial, spectroscopically prepared distribution, see the bottom panel in Figure 3. In the simulation we used a two exponential function for the solvation dynamics C(t),[1.b]

$$C(t) = A_1 \cdot \exp(-t/\tau_1) + A_2 \cdot \exp(-t/\tau_2). \tag{4-2}$$

These values for C(t) were measured by the transient Stokes–shift method, as discussed elsewhere.[1.b] The time–dependent diffusion coefficient which is used in the GSE simulations can be related to D(t). For C(t) of DMF $A_1 = 0.55$, $A_2 = 0.45$, $\tau_1 = 0.75$ ps, and $\tau_2 = 2.5$ ps.[1.b] Unfortunately, the experimental measurements of the transient fluorescence spectrum are not reliable over a broad enough wavelength region to allow for an accurate determination of A(t), the key observable for the determination of $S_G(t)$. We are in the process of improving the apparatus employed in these measurements in order to determine A(t) accurately. In this paper, however, we will emphasize the simulated A(t) data as shown in Figure 4. The simulated results (eqn 4–1) will allow us to demonstrate the physical significance of the $S_G(t)$ definition (eqn 2–33) and allow us to evaluate one of the important approximation (eqns 2–30 and 2–31).

Tominaga et al.[3] have demonstrated that the emission dynamics of ADMA at times > 150 fs is primarily due to emission from S_1. The time–dependent spectra (Figure 4)

reflect the continuously evolving probability distribution, $\rho_{S_1}(z,t)$, in S_1 as shown in Figure 3. Note that as the distribution shifts toward equilibrium (near z = 1) the emission intensity shifts toward lower frequency since the S_0/S_1 gap decreases as z goes from zero to one (Figure 3). In addition to shift in the spectrum as $\rho_{S_1}(z,t)$ evolves, the integrated area (Figure 5) also shows time–dependence. Simply speaking, as the average value of z increases from $0 \rightarrow 1$ the LE character of S_1 decreases, and, as a result, A(t) decreases because $\mu_{LE} > \mu_{CT}$. Note that the actual number of S_1 molecules is essentially constant during the evolution.[3]

Note also that $S_G(t)$ is not zero at infinite time, since the relaxed form of S_1 is not purely CT. Therefore, $S_G(\infty)$ has a finite value in eqn 2–23. $k_{et}(t)$ is portrayed in Figure 5. The time–dependence of $k_{et}(t)$ reflects three complex effects, namely the dependence of $C_{LE}^{(1)}(z)$ on z, the anharmonic shape of $F_{S_1}(z)$ at the initially prepared z values, and complex diffusion effects due to the time–dependent diffusion coefficient D(t), as shown in Figure 4. Nevertheless, a unique value for the et rate constant can be obtained by determining the limiting rate coefficient k_{et}^{lim}.

The generalized survival during the S_1 evolution is shown in Figure 5. This shows that the survival probability indeed decreases as the S_1 adiabatic et process occurs. The value we extract for ADMA from the simulation is $k_{et}^{lim} = 1/(2.50\ ps)$. k_{et}^{lim} is equal to the inverse of the slower solvation time τ_2. This is precisely the result expected in the limit discussed in Section 3, where the potential is approximately given $F_{CT}(z)$ in the equilibrium region of S_1 *and* the solvation dynamics are characterized by C(t) of the form of eqn 4–2.

Figure 6 provides a comparison of the survival $S_G(t)$ and hence $k_{et}(t)$ calculated two ways. The middle panel shows $k_{et}(t)$ calculated "exactly" from eqn 2–23. Alternatively, we can determine $S_G(t)$ from the simulated area using the approximate result which connects experiment and $S_G(t)$ (eqn 2–26). The upper panel shows $k_{et}(t)$ resulting from a simulation

of $S_G(t)$. For the both cases a two exponential form for the solvation was used. While the exact and approximate results are not identical, the approximate approach is reasonably accurate, especially at longer times, supporting the validity of the approximation of eqns 2–30 and 2–31.

It should be strongly emphasized that while $k_{et}(t)$ can be simply related to A(t), there is no simple relationship between $k_{et}(t)$ and the emission dynamics $I(\nu,t)$ at *any* single emission wavelength. This is an important result which impacts on the interpretation of published data on the transient fluorescence data of ADMA and related molecules.

The bottom panel in Figure 6 shows "exact" $k_{et}(t)$ (eqns 2–18 and 2–23) for a solvent with a single solvent relaxation time τ_s = 1.5 ps. All other parameter are identical to the simulation results in Figure 4 and the middle panel of Figure 6. At long times $k_{et}(t)$ is well characterized by the inverse of a single solvation time, with a limiting rate coefficient k_{et}^{lim} = 1/(1.5 ps), in accord with simple results of Section 3.

The overall shape of $k_{et}(t)$, as time increases, is qualitatively similar for the single exponential and bi–exponential solvation dynamics. There is a prompt increase in $k_{et}(t)$ at early times (barely observable in Figure 6), a slower decay of $k_{et}(t)$, and finally a limiting value. The early time increase is due to the increase in the magnitude of $dF_{S_1}(z)/dz$ as z increases, which accelerates the diffusion. The intermediate rate coefficient decrease is apparently due to the strong dependence of $C_{LE}^{(1)}(z)$ on z as shown in Figure 3.

5. The Electron Transfer Kinetic of BA

The et mechanism of BA is different from that of ADMA in two important ways. First, there are two CT states which should be considered (Figure 7). Second, the adiabatic S_1 et mechanism in polar solvent of BA involves a small barrier ($\Delta F^{\ddagger} \sim 0.5$ kcalmol^{-1}) between the reactant "well" and product "wells" (Figure 8), while for ADMA the reaction is

barrierless in S_1.

The appropriate equations for the three adiabatic excited BA are summarized by the following.

$$|S_1\rangle = C_{CT}^{(1)}(z)|CT'\rangle + C_{LE}^{(1)}(z)|LE\rangle + C_{CT}^{(1)}(z)|CT\rangle. \qquad (5\text{–}1)$$

$$|S_2\rangle = C_{CT}^{(2)}(z)|CT'\rangle + C_{LE}^{(2)}(z)|LE\rangle + C_{CT}^{(2)}(z)|CT\rangle. \qquad (5\text{–}2)$$

$$|S_3\rangle = C_{CT}^{(3)}(z)|CT'\rangle + C_{LE}^{(3)}(z)|LE\rangle + C_{CT}^{(3)}(z)|CT\rangle. \qquad (5\text{–}3)$$

For BA laser excitation at 400 nm prepares the S_1 state exclusively. The time–dependence of $\rho_{S_1}(z,t)$ has been simulated as shown in Figure 9. The upper panel portrays the recently published GLE simulation of $\rho(z,t)$ in the overdamped limit using the following solvation parameters for C(t): $A_1 = 0.46$, $A_2 = 0.54$, $\tau_1 = 0.43$ ps, and $\tau_2 = 4.1$ ps. $\rho(z,t)$ is calculated from z(t) trajectories calculated by the GLE. The lower panel of Figure 9 shows a GSE simulation of $\rho(z,t)$ using the same initial conditions and solvation parameter as the GLE calculation. The evolution of $\rho(z,t)$ according to the GSE is noticeably slower (roughly a factor of 2). It has been noticed in other contexts that the GSE leads to slower (and apparently less accurate) dynamics.[17] In the present case, our goal is to explore the relationships between $k_{et}(t)$, A(t), $I(t,\nu)$, and $S_G(t)$, rather than explore the relationship between $k_{et}(t)$ and the solvation dynamics, so we emphasize GSE calculations which are computationally less expensive. Note that the small barrier between the reactant and products is large enough to maintain a reactant peak in $\rho_{S_1}(z,t)$. This separation of $\rho_{S_1}(z,t)$ into different regions coupled with the S_1/S_0 energy gap dependence due to the reaction barrier, causes the simulated spectra to be approximately the sum of separate "reactant"

and "product" bands, see Figure 10.

The presence of even a small barrier, as in the case of BA, is apparently sufficient to dramatically alter the spectral manifestations of the et kinetics. See, in particular, in Figure 11 the dynamics of the survival $S_G(t)$ ("exact", see eqns 2–18 and 2–23), the spectral area A(t), and the intensity dynamics I(t,413nm) at the "blue edge" emission wavelength. All these are very similar. Thus, either experimental observable A(t) or $I(t,\nu)$ gives a reasonably accurate measurement of $S_G(t)$. For example, the half–lifetime of $S_G(t)$ in Figure 11 is 3.0 ps, while the corresponding values for A(t) and I(t, 413nm) are 3.3 and 3.1 ps, respectively. This demonstrates that the existence of even a small barrier can simplify the measurement of adiabatic et kinetics, for $k_{et}(t)$ by essentially producing a "reactant" region of the emission spectrum. This is analogous to the large barrier limit of the strongly adiabatic regime, which resembles transition–state–theory. In this limit the survival is defined for BA as

$$S_{TST} = \int_{-z_c}^{+z_c} dz \rho_{S_1}(z,t), \qquad (5–1)$$

where z_c and $-z_c$ are the locations of the dividing points separating the reactant and products wells. In an earlier paper we demonstrated that $S_{TST}(t)$ was nearly indistinguishable from A(t) and I(t,413nm) for the BA simulations using the strongly adiabatic model.[4]

The fact that the probability distribution has separate peaks in the LE and CT regimes (due to the small barriers separating the LE and CT minima in $F_{S_1}(z)$) causes the approximation that $\overline{C_{LE}^{(1)\,2}(t)} \simeq \overline{(C_{LE}^{(1)}(t))^2}$ to be invalid. Consequently, the estimation of $k_{et}(t)$ from A(t) by eqn 2–26 for BA is in error and completely inappropriate.

From the standpoint of experimental measurements of $k_{et}(t)$ in terms of the strongly adiabatic model, it is essential that an extensive analysis be made for each molecules in order to classify the molecule in either the ADMA class (which has no barrier separating the reactant and product region) or the BA class (which possesses a barrier). The static absorption and fluorescence spectroscopy has features which should allow for a rapid classification for molecules that fall strongly in either class.[3,4] For molecules like BA the presence of the barrier ensures that $S_G(t)$ can be quantified directly from $I(t,\nu)$ in the blue edge of the fluorescence. For molecules that fall in the ADMA class, $A(t)$ must be measured experimentally in order to estimate $S_G(t)$ (using eqn 2–26) or alternatively $S_G(t)$ may be calculated "exactly" using eqns 2–18 and 2–23.

5. Conclusions and Summary

The recently introduced phenomenological model for strongly adiabatic et in the excited states of aromatic electron donor/acceptor compounds has been developed in more detail. The underlying assumptions in the model have been delineated. A definition of a generalized reactant survival probability $S_G(t)$ has been given. An expression relating $S_G(t)$ and the experimental observable $A(t)$, the integrated emission intensity has been derived. The utility of these approaches have been applied to the photodynamics of BA and ADMA, using the previously estimated free energy versus solvent coordinate dependencies of these compounds in typical organic solvents. The general applicability of the strongly adiabatic model has been discussed.

Acknowledgements

We gratefully acknowledge support from the Office of Naval Research for this research.

References

1. For recent reviews on excited state et, see (a) Simon, J. D. *Acc. Chem. Res.* **1988**, 21, 128. (b) Barbara, P. F.; Jarzeba, W. *Adv. Photochem.* **1990**, 15, 1. (c) Maroncelli, M.; MacInnis, J.; Fleming, G. R. *Science* **1988**, 243, 1674. (d) Lippert, E.; Rettig, W.; Bonačić–Koutecký, V.; Heisel, F.; Miehé, J. A. *Adv. Chem. Phys.* **1987**, 68, 1.
2. Okada, T.; Fujita, T.; Mataga, N. *Z. Phys. Chem. N. F.* **1976**, 101, 57. Okada, T.; Mataga, N.; Baumann, W.; Siemiarczuk, A. *J. Phys. Chem.* **1987**, 91, 4490. Mataga, N.; Nishikawa, S.; Asahi, T.; Okada, T. *J. Phys. Chem.* **1990**, 94, 1443. Chandross, E. A. in *The Exciplex*, Gordon, M., Ware, W. R., eds.; Academic: New York, 1975; p 187. Siemiarczuk, A.; Grabowski, Z. R.; Krówczyński, A.; Asher, M.; Ottolenghi, M. *Chem. Phys. Lett.* **1977**, 51, 315. Grabowski, Z. R.; Rotkiewicz, K.; Siemiarczuk, A. *J. Luminescence* **1979**, 18/19, 420. Grabowski, Z. R.; Rotkiewicz, K.; Siemiarczuk, A.; Cowley, D. J.; Baumann, W.; *Nouv. J. Chim.* **1979**, 3, 443. Siemiarczuk, A.; Koput, J.; Pohorille, A. *Z. Naturforsch.* **1982**, 37a, 598. Baumann, W.; Petzke, F.; Loosen, K.–D. *Z. Naturforsch.* **1979**, 34a, 1070. Detzer, N.; Baumann, W.; Schwager, B.; Fröhling, J.–C.; Brittinger, C. *Z. Naturforsch.* **1987**, 42a, 395. Rollinson, A. M.; Drickamer, H. G. *J. Chem. Phys.* **1980**, 73, 5981. Nagarajan, V.; Brearley, A. M.; Kang, T. J.; Barbara, P. F. *J. Chem. Phys.* **1987**, 86, 3183. Huppert, D.; Rentzepis, P. M. *J. Phys. Chem.* **1988**, 92, 5466.
3. Tominaga, K.; Walker, G. C.; Jarzeba, W.; Barbara, P. F. preceding paper in this issue.
4. Kang, T. J.; Jarzeba, W.; Barbara, P. F.; Fonseca, T. *Chem. Phys.* **1990**, 149, 81.
5. Hopfield, J. *Proc. Natl. Acad. Sci. U.S.A.* **1974**, 71, 3640. DeVault, D.

Quantum–Mechanical Tunneling in Biological Systems, 2nd ed.; Cambridge University Press: Cambridge, 1984. Nonella, M.; Schulten, K. *J. Phys. Chem.* **1991**, 95, 2059. Warshel, A.; Chu, Z. T. *J. Chem. Phys.* **1990**, 93, 4003.

6. Hynes, J. T. *J. Phys. Chem.* **1986**, 90, 3701.
7. Rips, I.; Klafter, J.; Jortner, J. *J. Phys. Chem.* **1990**, 94, 8557.
8. Sumi, H.; Marcus, R. A. *J. Chem. Phys.* **1986**, 84, 4894.
9. Bagchi, B.; Fleming, G. R. *J. Phys. Chem.* **1990**, 94, 9.
10. For general reviews of et see: Marcus, R. A.; Sutin, N. *Biochem. Phys. Acta* **1985**, 811, 265. Newton, M. D.; Sutin, N. *Ann. Rev. Phys. Chem.* **1984**, 35, 437.
11. Kim, H. J.; Hynes, J. T. *J. Phys. Chem.* **1990**, 94, 2736. *J. Chem. Phys.* 1990, 93, 5194. *ibid* **1990**, 93, 5211.
12. Bader, J. S.; Chandler, D. *Chem. Phys. Lett.* **1989**, 157, 501. Bader, J. S.; Kuharski, R. A.; Chandler, D. *J. Chem. Phys.* **1990**, 93, 230.
13. By "approximate" we mean that we do not include a self–consistent treatment of solute electronic structure and solvent electronic polarization, see reference 11.
14. Beens, H.; Weller, A. *Chem. Phys. Lett.* **1969**, 3, 666.
15. Fonseca, T. *J. Chem. Phys.* **1989**, 91, 2869.
16. For example, see Wax, N. *Selected Papers on Noise and Stochastic Process*; Dover Publications: New York, 1954.
17. Fonseca, T. *Chem. Phys. Lett.* **1989** 162, 491.

Figure Captions

Figure 1. Molecular structures of bianthryl (BA) and 4–(9–anthryl)–N,N'–dimethylaniline (ADMA). Donor (D) and acceptor (A) signify the electron donor and acceptor chromophores, respectively. Schematic energy levels of the three relevant states in the non–polar solvent: ground state ($DA \equiv S_0$), locally excited state ($DA^* \equiv LE$) which results from the π–π^* excitation of the anthracene ring, and charge transfer state (D^+–$A^- \equiv CT$) which is an intramolecular ion–pair state.

Figure 2. Theoretical estimates for the (left) diabatic and (right) adiabatic free energies of ADMA in N,N'–dimethylformamide, as a function of the solvent coordinate. The free energy parameters are: $k_s = 13.0$ kcalmol^{-1}, $\Delta F^0 = 10.5$ kcalmol^{-1}, $H_{LE,CT} = 0.8$ kcalmol^{-1}. See ref. 3 and 4 for details of the simulation.

Figure 3. (upper panel) Theoretical estimate for the adiabatic S_1 surface of ADMA in N,N'–dimethylformamide. (middle panel) The square of the coefficient of the LE character in the adiabatic S_1 state, as a function of the solvent coordinate. (lower panel) Time–dependent probability distribution function on the S_1 surface of ADMA in N,N'–dimethylformamide obtained from a generalized Smoluchowski equation (GSE) and C(t) (eqn 4–2) with $A_1 = 0.55$, $A_2 = 0.45$, $\tau_1 = 0.75$ ps, and $\tau_2 = 2.5$ ps for the solvation dynamics. See ref. 3 for the details of the GSE simulation.

Figure 4. Simulation of the time–resolved emission spectra of ADMA in N,N'–dimethylformamide obtained from the probability distribution function on the adiabatic S_1 surface shown in Figure 3. The ratio of the transition dipole moment (μ_{CT}/μ_{LE}) (eqns 2–28 and 2–29) is 0.30 in the simulation.

Figure 5. (upper panel) The integrated emission intensity of the simulated time–resolved spectra (Figure 4) obtained from eqn 2–26 for ADMA in N,N'–dimethylformamide (DMF). (middle panel) The generalized survival ($S_G(t)$) for the adiabatic et reaction on the S_1 surface of ADMA in DMF obtained "exactly" from eqn 2–18. (lower panel) The generalized et rate coefficient obtained from eqn 2–23 and the generalized survival shown above.

Figure 6. (upper panel) The generalized et rate coefficient for the adiabatic et reaction on the S_1 surface of ADMA in N,N'–dimethylformamide obtained "approximately" from the integrated emission intensity and eqn 2–33 with the approximation of eqns 2–30 and 2–31. A two exponential function (eqn 4–2) with $A_1 = 0.55$, $A_2 = 0.45$, $\tau_1 = 0.75$ ps, and $\tau_2 = 2.5$ ps was used for the solvation dynamics. (middle panel) The generalized et rate coefficient obtained "exactly" from the generalized survival shown in Figure 5 and eqn 2–23. A two exponential function with the same parameters as above was used for the solvation dynamics. (lower panel) The generalized et rate coefficient obtained "exactly" from the eqn 2–23 and the probability distribution function (eqn 2–14). A single exponential function with $\tau_s = 1.5$ ps was used for the solvation dynamics.

Figure 7. Theoretical estimates for the (left) diabatic and (right) adiabatic free energies of BA in propylene carbonate as a function of the solvent coordinate. The free energy parameters are: $k_s = 21.0$ kcalmol^{-1}, $\Delta F^0 = 5.0$ kcalmol^{-1}, and $H_{LE,CT} = 1.0$ kcalmol^{-1}. See ref. 3 and 4 for details of the simulation.

Figure 8. (upper panel) Theoretical estimate for the adiabatic S_1 surface of BA in

propylene carbonate as a function of the solvent coordinate. (lower panel) The square of the coefficient of the LE character in the adiabatic S_1 state. The free energy parameters for both the panels are the same as those in Figure 7.

Figure 9. (upper panel) Time–dependent probability distribution function $\rho_{S_1}(z,t)$ on the S_1 surface of BA in propylene carbonate obtained from a generalized Langevin equation (GLE) and C(t) (eqn 4–2) with $A_1 = 0.46$, $A_2 = 0.54$, $\tau_1 = 0.43$ ps, and $\tau_2 = 4.1$ ps for the solvation dynamics. (lower panel) $\rho_{S_1}(z,t)$ for the same chemical obtained from a generalized Smoluchowski equation (GSE) and the same functional form as above for the solvation dynamics. See refs. 4 and 3 for details of the GLE and GSE simulations, respectively.

Figure 10. Simulation of the time–resolved emission spectra of BA in propylene carbonate obtained from the distribution function on the S_1 surface shown in the lower panel of Figure 8. A single exponential function of C(t) (eqn 4–2) with $\tau_s = 2.4$ ps was used for the solvation dynamics. The ratio of the transition dipole moments (μ_{CT}/μ_{LE}) (eqns 2–28 and 2–29) is 0.32 in the simulation.

Figure 11. (upper panel) The integrated emission intensity of the simulated time–resolved spectra (Figure 10) obtained from eqn 2–26 for BA in propylene carbonate (PC). (middle panel) The generalized survival ($S_G(t)$) for the adiabatic et reaction on the S_1 surface of ADMA in PC obtained "exactly" from eqn 2–18. (lower panel) The transient decay dynamics of the simulated emission spectra (Figure 10) at 413 nm ("the blue edge"). For all the panels a single exponential function of C(t) (eqn 4–2) with $\tau_s = 2.4$ ps was used to represent the solvation dynamics.

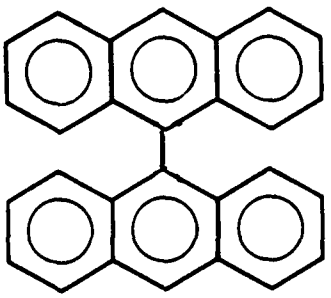

Donor

Acceptor

BA

$D^+A^- \equiv CT$

energy

$DA^* \equiv LE$

$DA \equiv S_0$

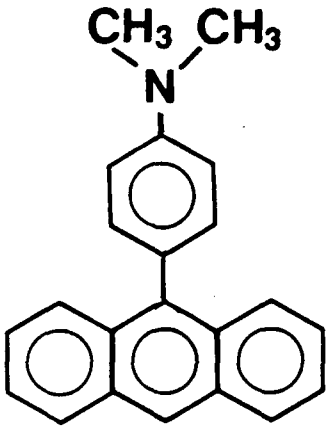

Donor

Acceptor

ADMA

Figure 1

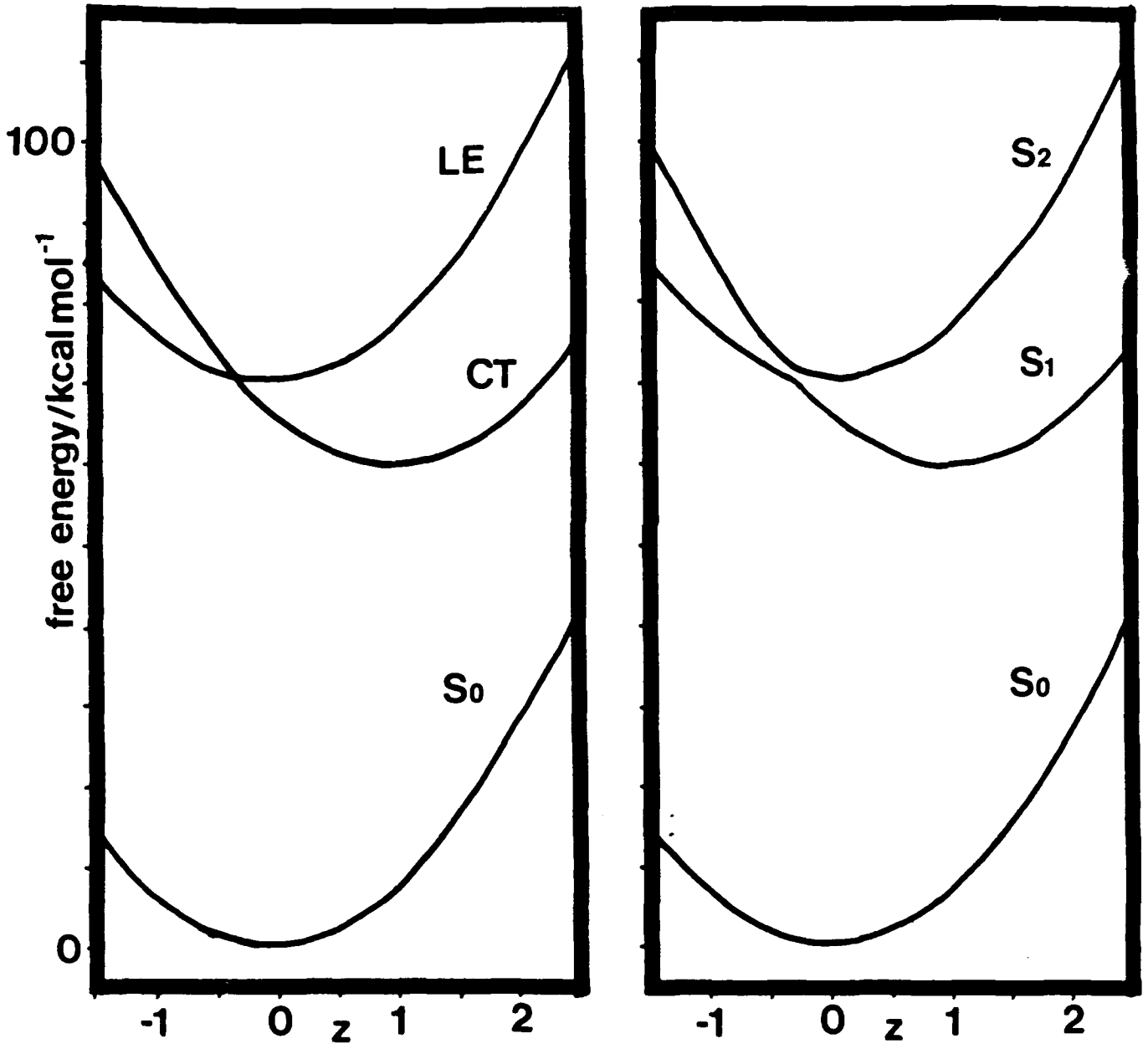

Figure 2

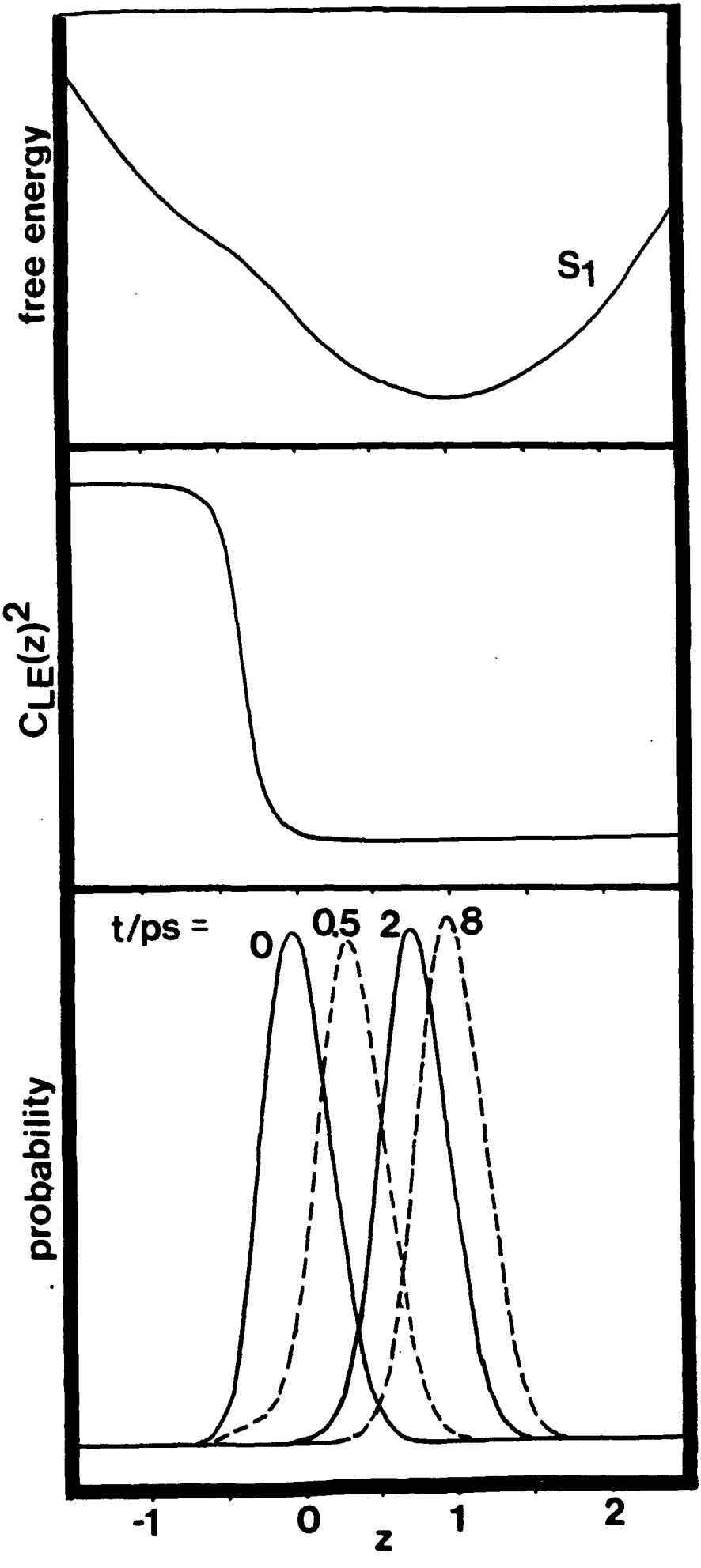

Figure 3

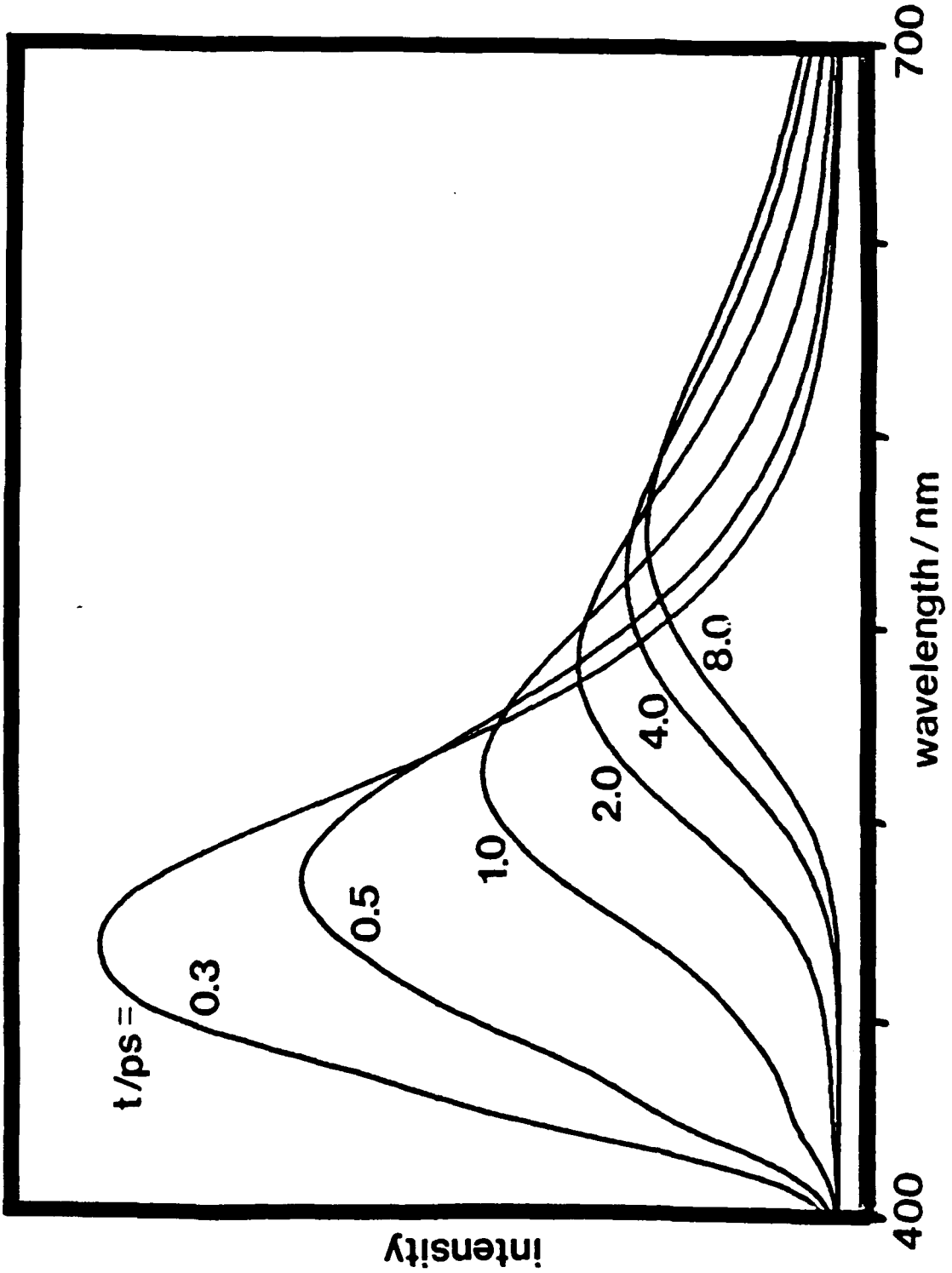

Figure 4

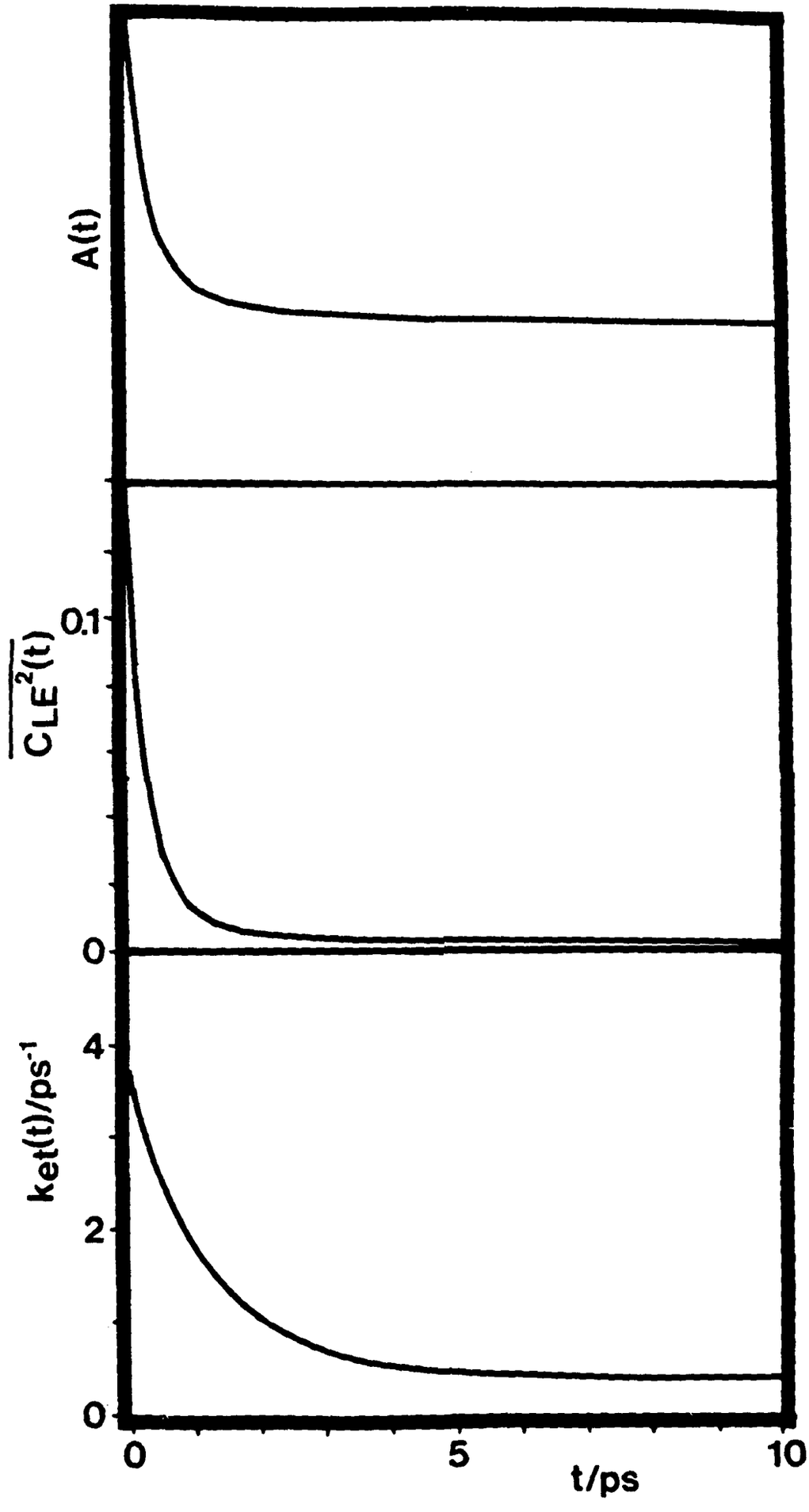

Figure 5

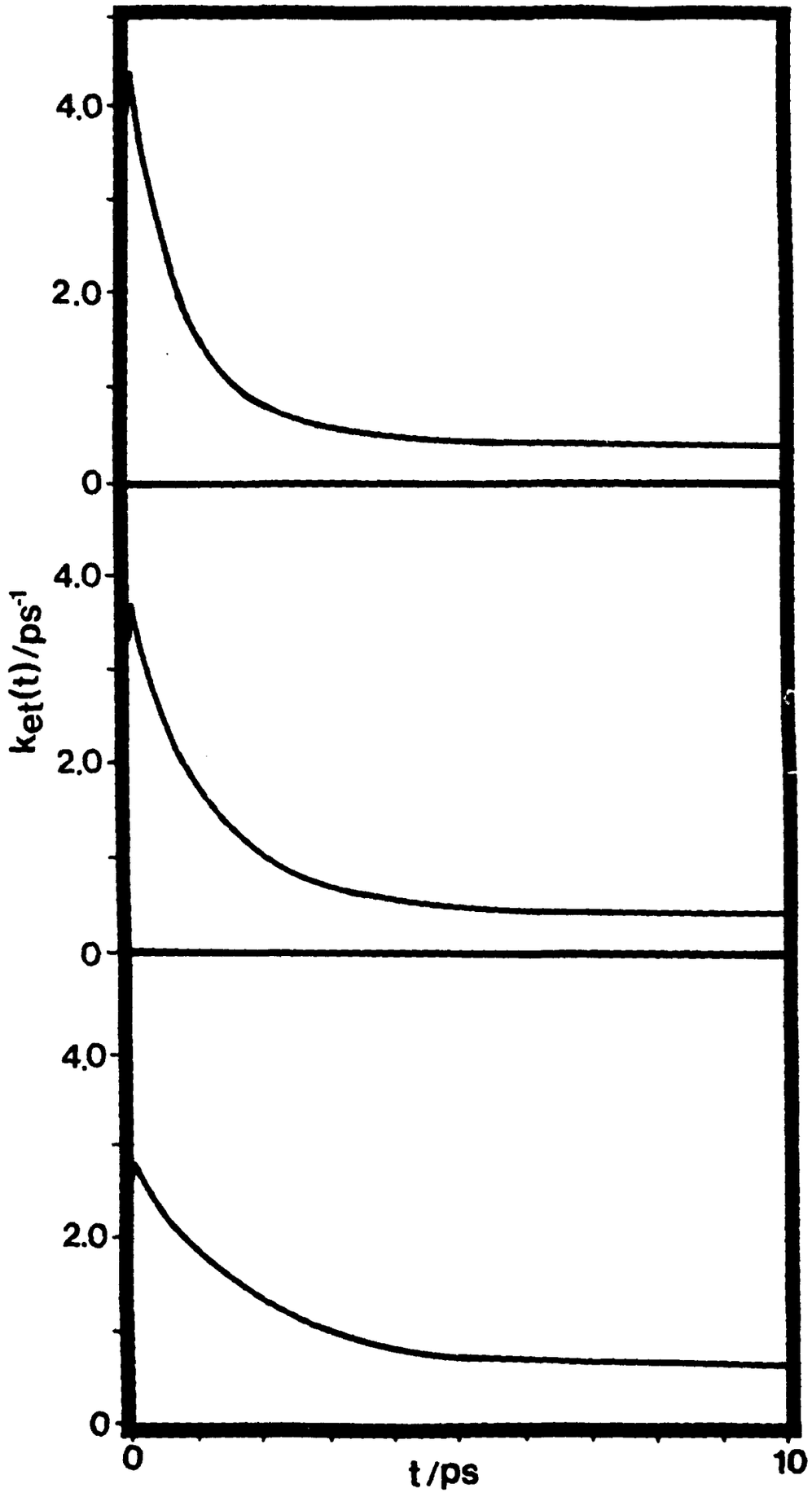

Figure 6

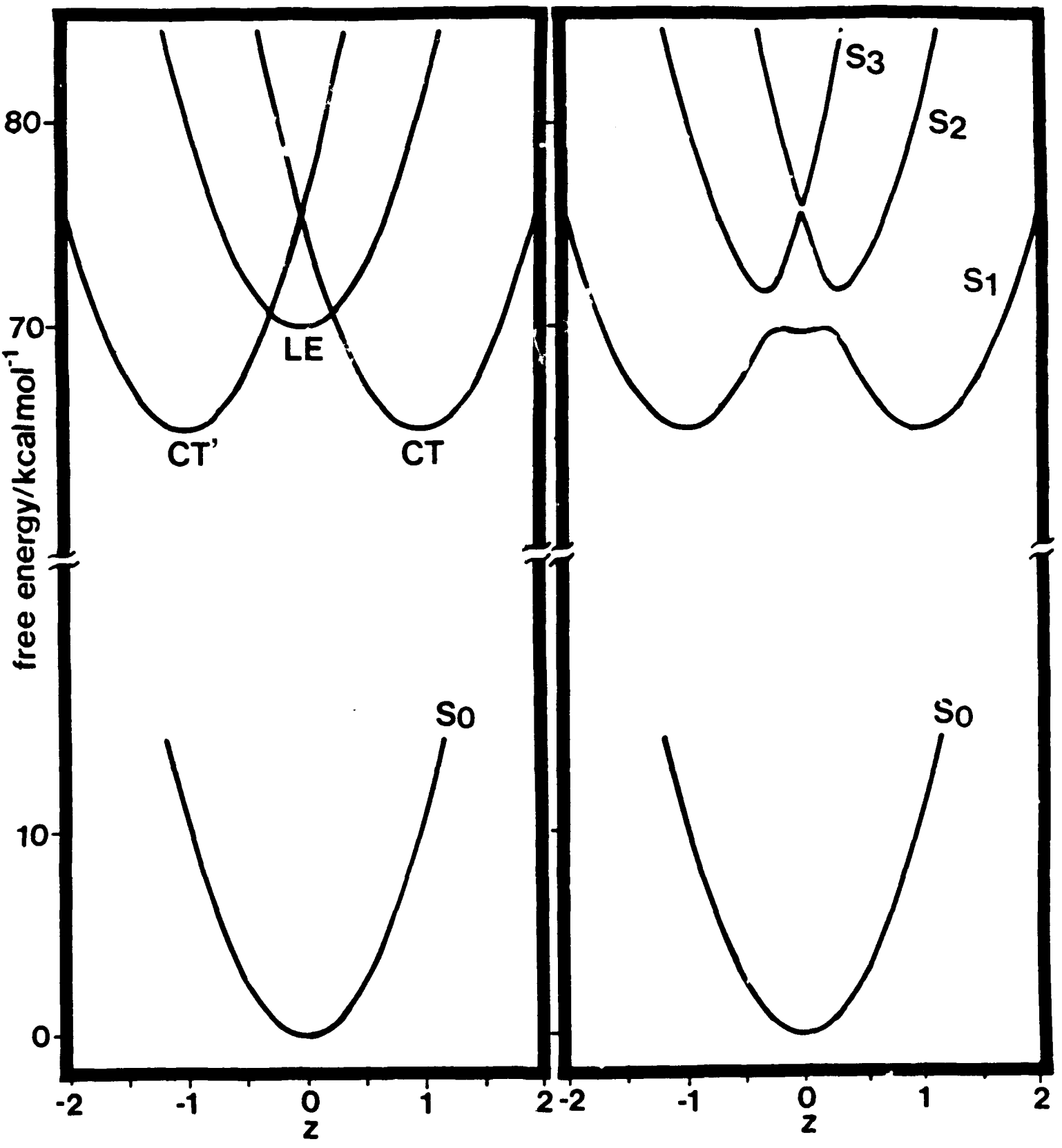
80
70
10
0
free energy/kcalmol^{-1}
CT'
LE
CT
S0
S3
S2
S1
S0
-2
-1
0
1
2
z
-2
-1
0
1
2
z

Figure 7

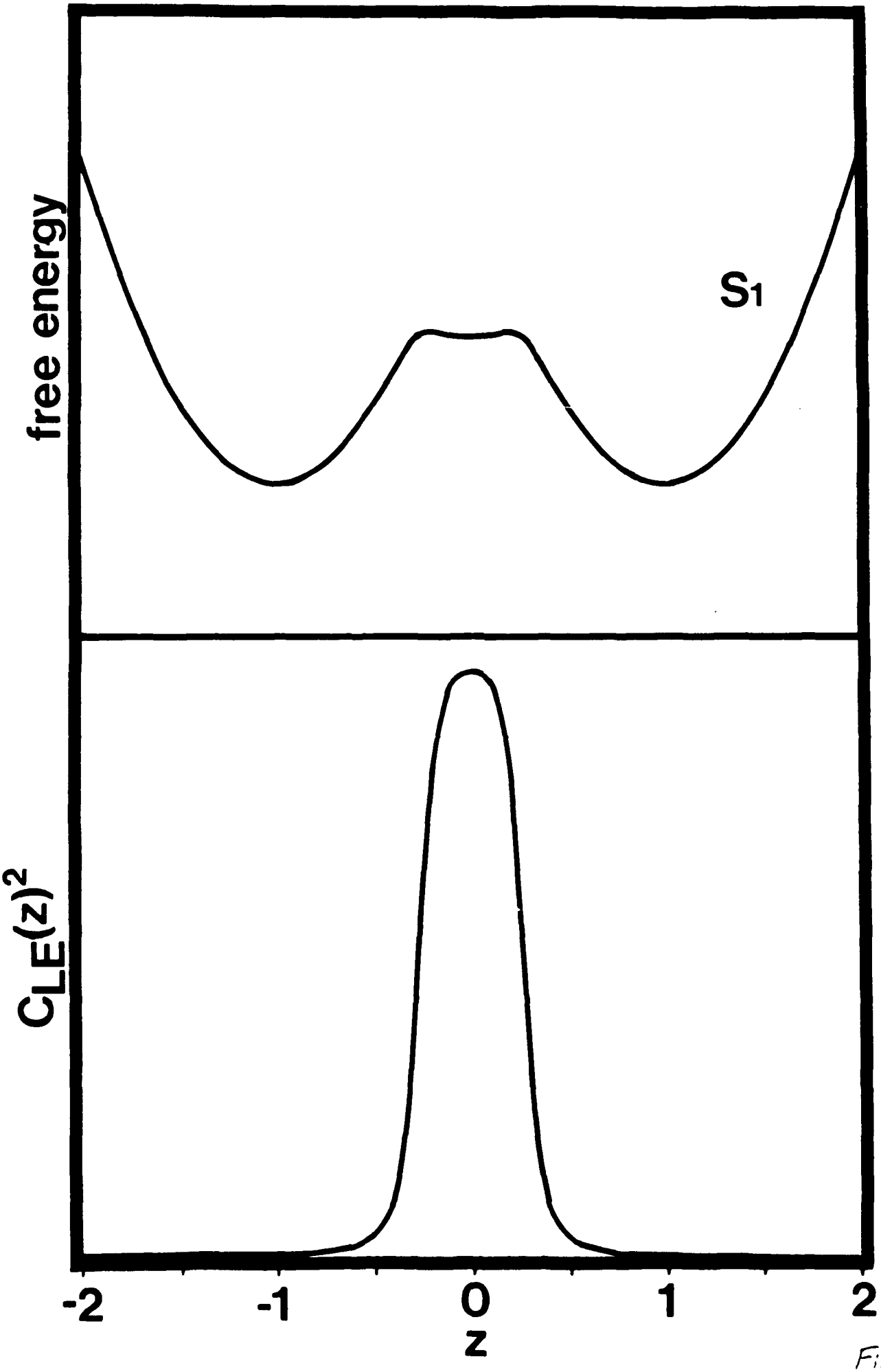

Figure 8

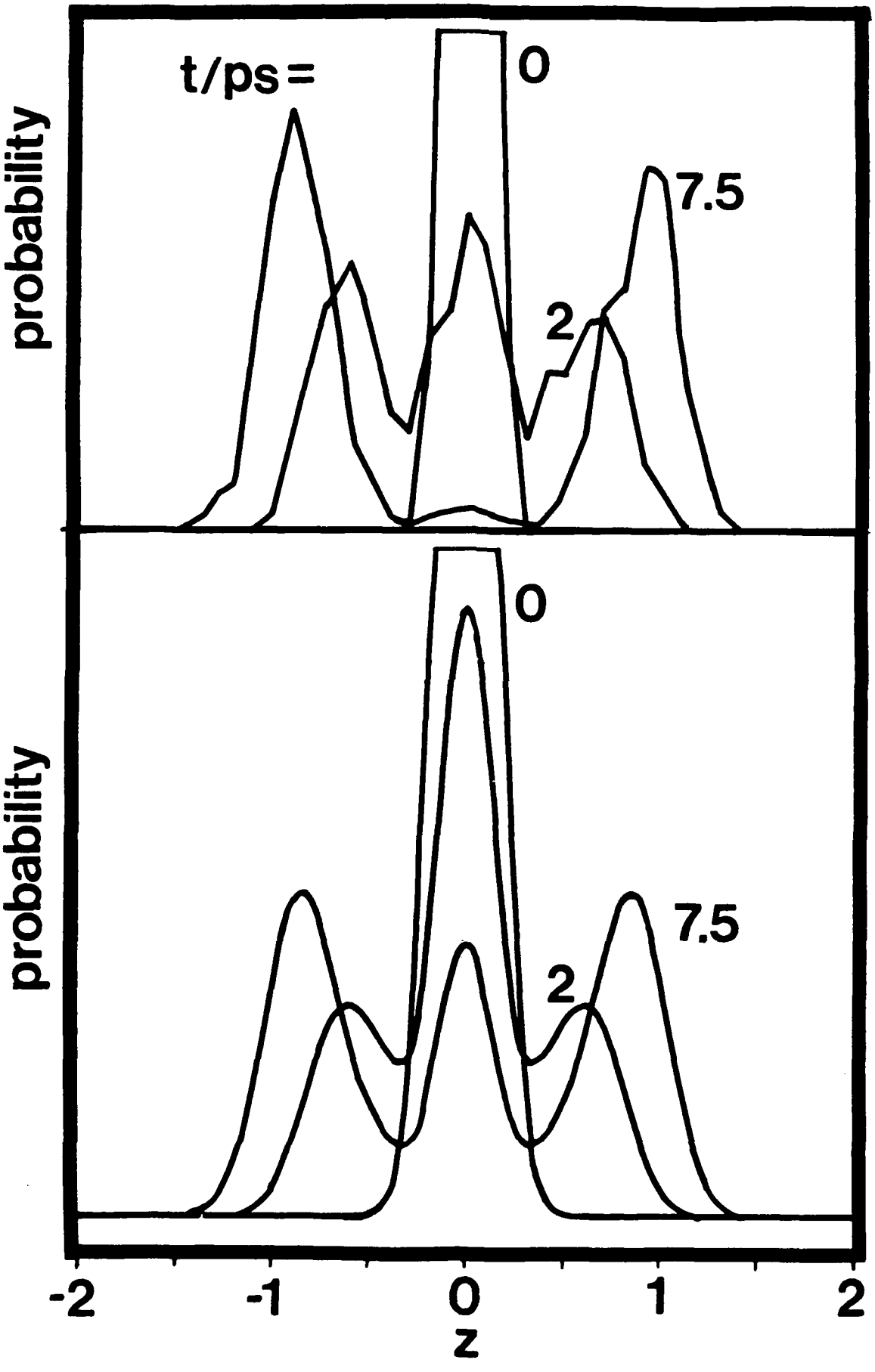

Figure 9

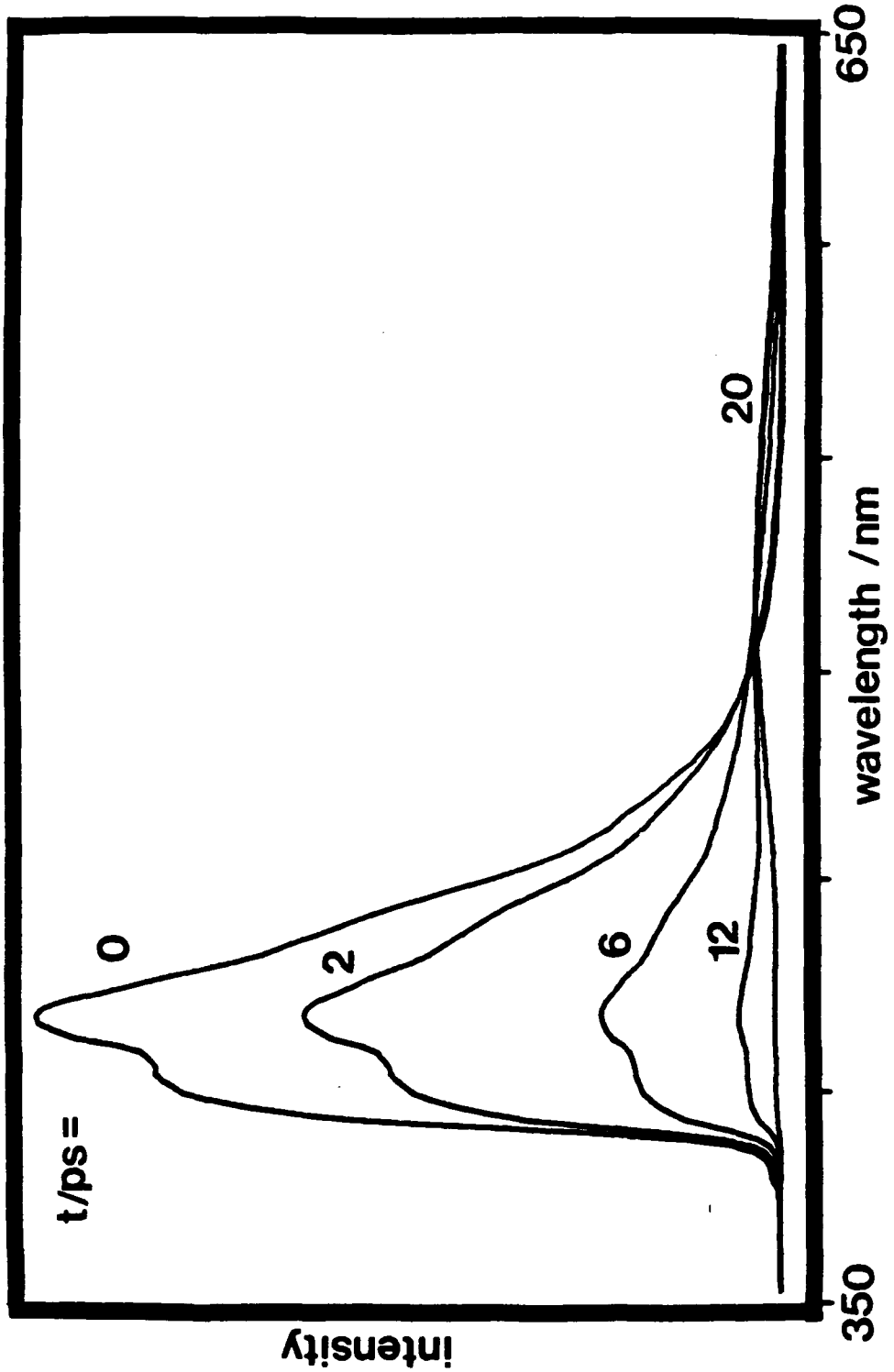

Figure 10

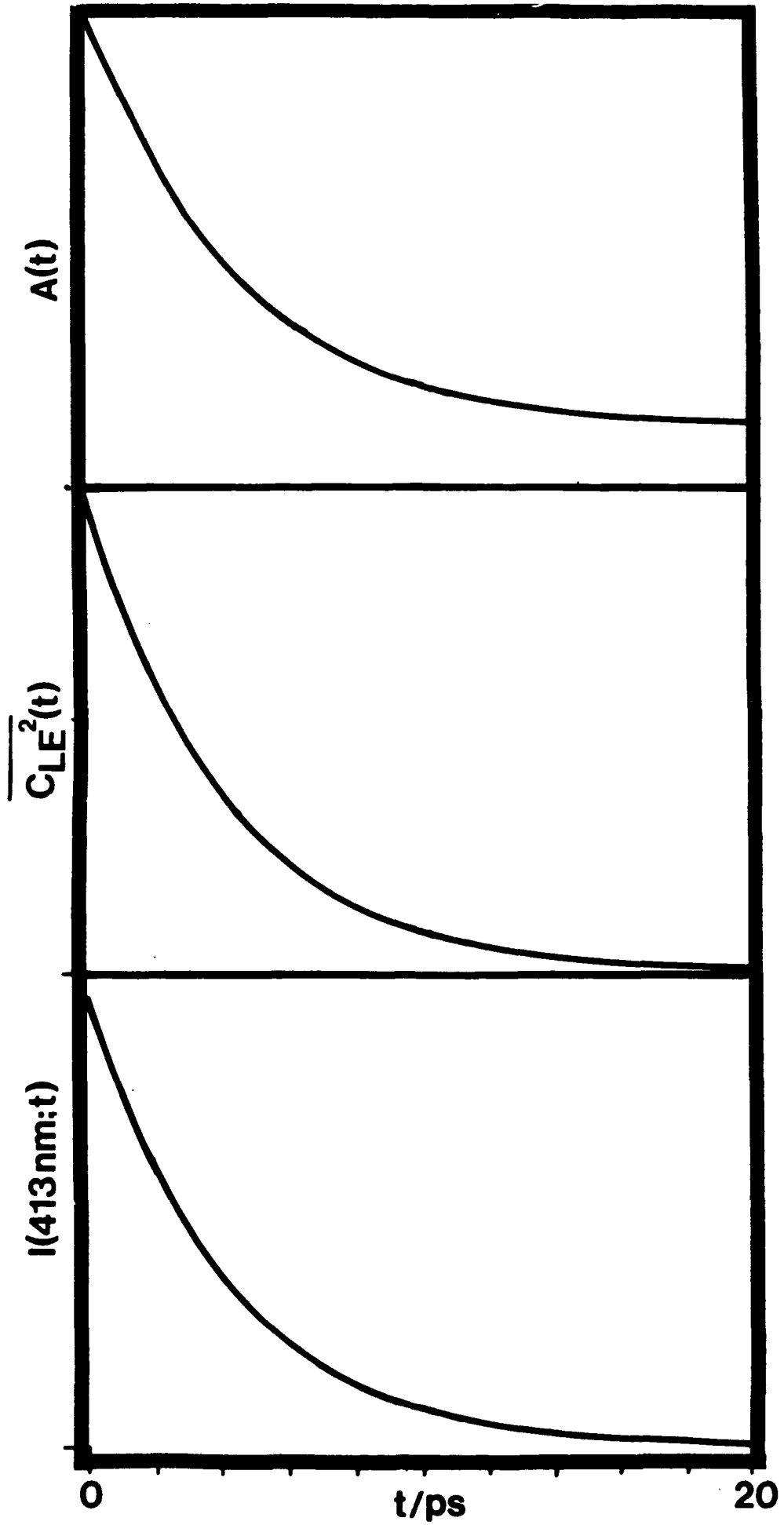

Figure 11

TECHNICAL REPORT DISTRIBUTION LIST - GENERAL

Office of Naval Research (2)*
Chemistry Division, Code 1113
800 North Quincy Street
Arlington, Virginia 22217-5000

Dr. James S. Murday (1)
Chemistry Division, Code 6100
Naval Research Laboratory
Washington, D.C. 20375-5000

Dr. Robert Green, Director (1)
Chemistry Division, Code 385
Naval Weapons Center
China Lake, CA 93555-6001

Dr. Eugene C. Fischer (1)
Code 2840
David Taylor Research Center
Annapolis, MD 21402-5067

Dr. Elek Lindner (1)
Naval Ocean Systems Center
Code 52
San Diego, CA 92152-5000

Commanding Officer (1)
Naval Weapons Support Center
Dr. Bernard E. Douda
Crane, Indiana 47522-5050

Dr. Richard W. Drisko (1)
Naval Civil Engineering
Laboratory
Code L52
Port Hueneme, CA 93043

Dr. Harold H. Singerman (1)
David Taylor Research Center
Code 283
Annapolis, MD 21402-5067

Chief of Naval Research (1)
Special Assistant for Marine
Corps Matters
Code 00MC
800 North Quincy Street
Arlington, VA 22217-5000

Defense Technical Information
Center (2)
Building 5, Cameron Station
Alexandria, VA 22314

* Number of copies to forward

Enclosure (2)